THE JOURNAL OF PHYSICAL CHEMISTRY Letters

Letter

pubs.acs.org/JPCL

New Insights in $4f^{12}5d^1$ Excited States of Tm^{2+} through Excited State Excitation Spectroscopy

Mathijs de Jong,[†] Daniel Biner,[‡] Karl W. Krämer,[‡] Zoila Barandiarán,[§] Luis Seijo,[§] and Andries Meijerink*[,†]

[†]Condensed Matter and Interfaces, Debye Institute for Nanomaterials Science, Utrecht University, Princetonplein 5, 3584 CC Utrecht, The Netherlands

[‡]Department of Chemistry and Biochemistry, University of Bern, 3012 Bern, Switzerland

[§]Departamento de Química, and Instituto Universitario de Ciencia de Materiales Nicolás Cabrera, Universidad Autónoma de Madrid, 28049 Madrid, Spain

Supporting Information

ABSTRACT: Optical excitation of ions or molecules typically leads to an expansion of the equilibrium bond lengths in the excited electronic state. However, for $4f^{n-1}5d^1$ excited states in lanthanide ions both expansion and contraction relative to the $4f^n$ ground state have been reported, depending on the crystal field and nature of the 5d state. To probe the equilibrium distance offset between different $4f^{n-1}5d^1$ excited states, we report excited state excitation (ESE) spectra for Tm^{2+} doped in $CsCaBr_3$ and $CsCaCl_3$ using two-color excited state excitation spectroscopy. The ESE spectra reveal sharp lines at low energies, confirming a similar distance offset for $4f^{n-1}5d(t_{2g})^1$ states. At higher energies, broader bands are observed, which indicate the presence of excited states with a different offset. On the basis of ab initio embedded-cluster calculations, the broad bands are assigned to two-photon d−d absorption from the excited state. In this work, we demonstrate that ESE is a powerful spectroscopic tool, giving access to information which cannot be obtained through regular one-photon spectroscopy.

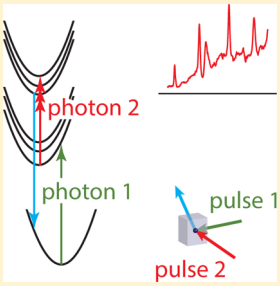

The luminescence of lanthanide (Ln) ions doped in crystalline solids has been widely investigated. Both intraconfigurational $4f^n \leftrightarrow 4f^n$ (f−f) as well as interconfigurational $4f^n \leftrightarrow 4f^{n-1}5d^1$ (f−d) transitions find application in a wide range of luminescent materials for lighting, displays, medical imaging, homeland security, biomarkers, afterglow, lasers, and more.[1−6] The characteristic sharp line spectra of f−f transitions are well-understood. For the broad band spectra arising from f−d transitions, the fundamental insight is not as complete and important questions remain open, for example, on nonradiative decay (quenching) processes from $4f^{n-1}5d^1$ (fd) states. For understanding nonradiative relaxation between excited states and relaxation to the ground state, the change in the equilibrium distance between the Ln cation and surrounding anions for the various states involved is crucial.[7,8]

Previous work has revealed that for fd excited states both expansion and contraction relative to the $4f^n$ ground state can occur, depending on the nature of the state of the 5d electron in the fd states.[9] In one-photon excitation spectra both contraction or expansion in the excited state gives rise to vibrationally broadened bands and no information is obtained on the direction of the change in bond length associated with the electronic transition.[10]

In order to probe the variation in equilibrium distance for different excited states, a powerful tool would be to measure absorption spectra for transitions between excited states. Electronic transitions between two excited states with a similar distance offset (either contraction or expansion) will show sharp line spectra, whereas transitions between contracted and expanded excited states will result in a broad band. The most sensitive technique to measure absorption is excitation spectroscopy. However, to measure excitation from a lower excited state to higher excited states, it is crucial that emission can be observed from a higher excited state. The situation is schematically depicted in the configuration coordinate diagram (CCD) in Figure 1, which gives the energy of excited states as a function of the vibrational coordinate (ion-ligand distance). In an excited state excitation process, the first photon (green line in Figure 1) excites the system to the lowest excited state. A second photon, resonant with the energy difference between the lowest and higher energy excited states (red lines in Figure 1) can bring the system to a higher energy state. By monitoring the (anti-Stokes) emission from the emitting high energy state (long blue line in Figure 1) as a function of the energy of the second photon, an excited state excitation (ESE) spectrum is obtained, giving information on the nature of the transition between different excited states.

For f−f transitions of Ln-ions and d−d transitions of transition metal ions, a small number of ESE spectra have been reported, for example, aimed at revealing high energy $4f^n$ levels in the vacuum UV or to obtain insight in mismatches for energy

Received: April 29, 2016
Accepted: June 27, 2016
Published: June 27, 2016

DOI: 10.1021/acs.jpclett.6b00924
J. Phys. Chem. Lett. 2016, 7, 2730−2734

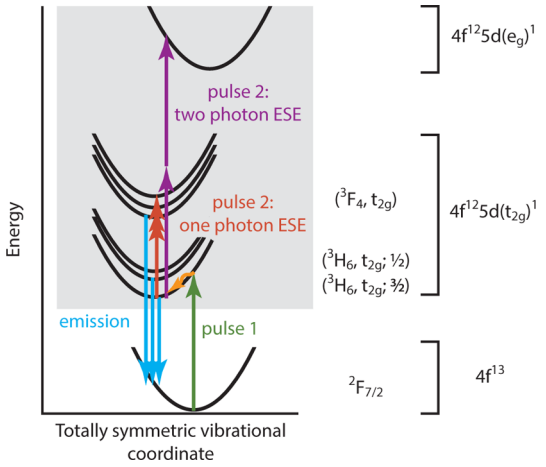

Figure 1. Schematic configuration coordinate diagram (CCD) of a two-color excited state excitation experiment in Tm^{2+}. The experiment starts with a photon from a first laser pulse (green line), bringing Tm^{2+} in the lowest excited $4f^{12}5d^1$ state. A second photon (red lines), of which the energy can be varied, will excite the ion to higher excited $4f^{12}5d^1$ states while the $(^3F_4, t_{2g})$ emission (long blue line) is probed. The excited state excitation (ESE) spectrum is measured by varying the energy of the second photon. The gray area is the part of the CCD that is calculated in Figure 4.

transfer in upconversion processes.[11−16] For f−d transitions, only a few ESE experiments have been reported focused on probing mid-infrared transitions between fd states and trapped exciton states.[17] ESE spectra on f−d transitions are hard to realize, as emission from fd states at energies higher than the lowest fd state is extremely rare. In almost all cases, there is rapid relaxation to the lowest fd state which is the only emitting fd state. In the recent literature, a few exceptions can be found. In 2005 it was shown that Tm^{2+} ($4f^{13}$) doped in $CsCaBr_3$ shows emission from three different $4f^{12}5d^1$ excited states.[18]

Here, we report $4f^{12}5d^1 \rightarrow 4f^{12}5d^1$ excited state excitation spectra for Tm^{2+} in $CsCaBr_3$ and $CsCaCl_3$ aimed at probing the variation in equilibrium distance between different $4f^{12}5d^1$ states. The $4f^{12}5d^1$ configuration consists of 910 states and therefore Tm^{2+} shows a rich absorption spectrum with many absorption bands. The excited $4f^{12}5d^1$ configuration can in first approximation be described in terms of the state of the $4f^{12}$ core and the state of the 5d electron. The lowest excited state for Tm^{2+} in octahedral O_h coordination is described as $(^3H_6, t_{2g})$, $^3H_6$ being the ground state for the $4f^{12}$ configuration and t_{2g} being the lower energy crystal field component for the 5d electron in octahedral coordination. In addition, interaction between the $S = 1$ spin of the $^3H_6$ state and the $S = 1/2$ spin of the 5d electron can give rise to a high spin (HS) $S = 3/2$ and a low spin (LS) $S = 1/2$ splitting for the lowest excited state. The HS state $(^3H_6, t_{2g}; 3/2)$ is lowest in energy, followed at higher energies by states of mixed HS and LS character, which we label as $(^3H_6, t_{2g}; 1/2)$. Because of stronger mixing of the higher energy fd states, S ceases to be a good quantum number and is therefore not included in the label for the $(^3F_4, t_{2g})$ state.[18]

Three emitting $4f^{12}5d^1$ states (see blue lines in Figure 1) have been identified for Tm^{2+} in $CsCaBr_3$ by Grimm et al. and assigned to (1) $(^3H_6, t_{2g}; 3/2)$, (2) $(^3H_6, t_{2g}; 1/2)$ and (3) $(^3F_4, t_{2g})$. To allow emission from higher energy $4f^{12}5d^1$ states, nonradiative relaxation from the higher fd states has to be suppressed. This can be achieved if the potential energy surfaces (PESs) of the excited states in the CCD of Figure 1 are parallel.[8] In addition, the energy gap to the next lower excited state should be large and the phonon energy low to prevent fast multiphonon relaxation. These conditions are met for Tm^{2+} in $CsCaBr_3$ and $CsCaCl_3$, allowing the observation of emission from the $(^3F_4, t_{2g})$ excited state. This makes it possible to perform ESE experiments. In this Letter we present ESE spectra for Tm^{2+} in both $CsCaBr_3$ and $CsCaCl_3$ from the $4f^{12}5d^1$ $(^3H_6, t_{2g}; 3/2)$ excited state, in which there is the unique possibility of both observing intraconfigurational f−f and d−d transitions. Sharp features in the spectra demonstrate that the

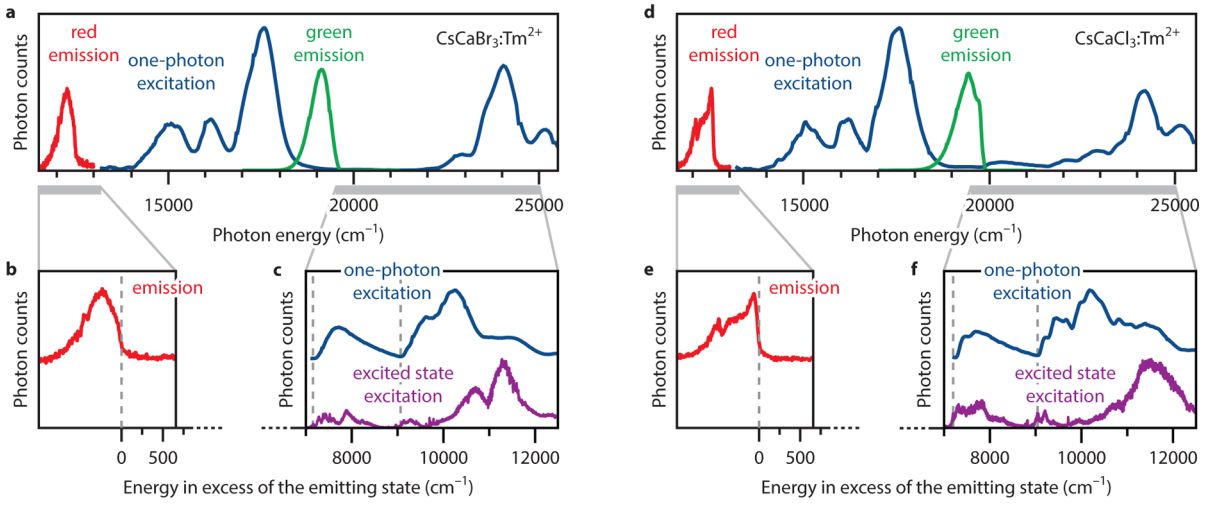

Figure 2. Comparison between the one-photon and excited state excitation spectra in $CsCaBr_3:Tm^{2+}$ (a−c) and $CsCaCl_3:Tm^{2+}$ (d−f). In (a) and (d), the emission (red lines for the $(^3H_6, t_{2g}; 3/2)$ emission, green lines for the $(^3F_4, t_{2g})$ emission) and one-photon excitation spectra (blue lines, recorded for the red emission) are plotted on a regular energy axis. In (b,c) and (e,f) the energy axes are shifted by the energy of the lowest $(^3H_6, t_{2g}; 3/2)$ state to allow comparison between the one-photon excitation spectra (blue lines, recorded for the green emission) and the excited state excitation spectra (purple lines). The shift was determined by taking the onset of the $(^3H_6, t_{2g}; 3/2) \rightarrow {}^2F_{7/2}$ emission bands (dashed gray lines). In this way, the position of the peaks in the excited state excitation spectrum should correspond with bands in the regular one-photon excitation spectrum. Full experimental details can be found in the text and Supporting Information.

DOI: 10.1021/acs.jpclett.6b00924
J. Phys. Chem. Lett. 2016, 7, 2730−2734

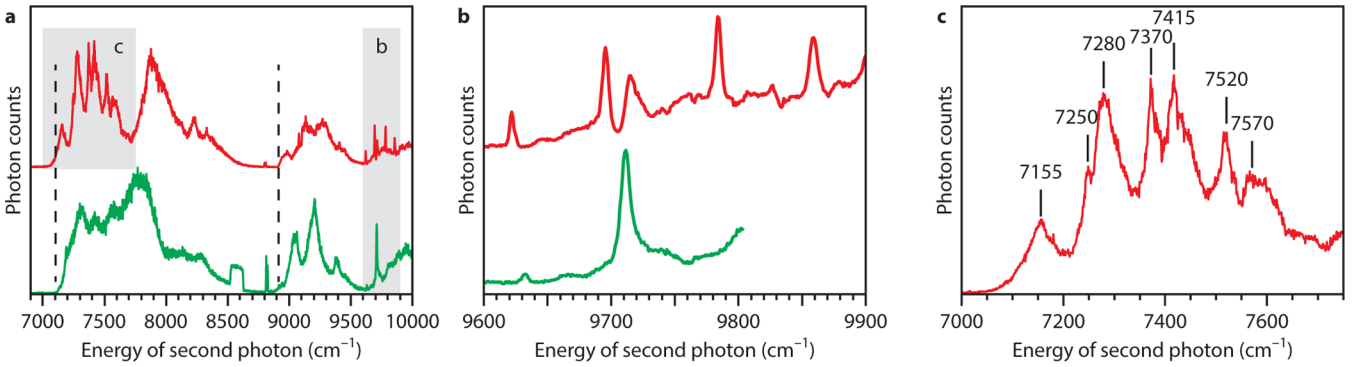

Figure 3. High-resolution excited state excitation spectra of $CsCaBr_3:Tm^{2+}$ (red) and $CsCaCl_3:Tm^{2+}$ (green). The gray areas in (a) indicate the details shown in (b) and (c). Because $CsCaCl_3:Tm^{2+}$ did not show sharp peaks between 9800 and 9900 cm^{-1} in (a), that range was not measured at high resolution in (b).

PESs of the different $4f^{12}5d(t_{2g})^1$ excited states are parallel, that is, have the same equilibrium distance. At higher energies, broad bands appear in the ESE, and they are assigned to two-photon absorption by transitions to ($^3H_6$, t_{2g}/e_g) mixed states.

The measurements of ESE spectra were performed on single crystals of $CsCaBr_3:Tm^{2+}$ 0.5 mol % and $CsCaCl_3:Tm^{2+}$ 1 mol %. The crystals were cooled down to 4 K with an Oxford Instruments liquid helium flow cryostat, because the ($^3F_4$, t_{2g}) high energy emission of Tm^{2+} is quenched at elevated temperatures. The ESE spectra were measured using two tunable optical parametric oscillator (OPO) lasers. Excitation in the lowest $4f^{12}5d^1$ state was done with an Ekspla NT 342B laser (at 13 158 cm^{-1} for $CsCaBr_3:Tm^{2+}$ and 13 072 cm^{-1} for $CsCaCl_3:Tm^{2+}$) and the second laser pulse of varying energy was from an Opotek Opolette HE 355II laser coupled into an optical fiber. To realize high resolution ESE spectra, the step size was 0.1 nm. For emission detection, a 0.55 m Triax 550 monochromator and a Hamamatsu R928 photomultiplier tube (PMT) were used. The PMT signal was analyzed in photon counting mode with a Stanford Research SR400 gated photon counter. The timing of the laser pulses was controlled with a Stanford Research DG535 pulse generator. A 100 μs delay between the pulses was used to suppress the detection of anti-Stokes emission due totwo-photon absorption within the first laser pulse. The emission was collected for a gate width of 10 μs immediately after the second laser pulse. A more complete description of the experimental details and the results of two control experiments can be found in the Supporting Information.

To record ESE spectra, the energy of the second laser pulse was varied between 12 500 and 6897 cm^{-1}. In Figure 2c,f, the ESE spectra for the green ($^3F_4$, t_{2g}) emission are shown for Tm^{2+} in $CsCaBr_3$ and $CsCaCl_3$ (purple lines). The ESE spectra are plotted together with the one-photon excitation (OPE) spectra. The axis of the ESE spectra is shifted relative to the axis of the OPE spectra by an energy corresponding to the zero-phonon line (ZPL) position of the lowest energy ($^3H_6$, t_{2g}; 3/2) state from which the ESE starts. This allows direct comparison of features observed in the ESE and OPE spectra. As no sharp zero-phonon lines are observed in excitation or emission, the ZPL position is estimated from the onset of the ($^3H_6$, t_{2g}; 3/2) emission bands: 12 510 cm^{-1} for $CsCaBr_3:Tm^{2+}$ and 12 580 cm^{-1} for $CsCaCl_3:Tm^{2+}$. The positions of the excitation bands in OPE and ESE are in good agreement (see dashed lines) and confirm that the bands observed in the ESE spectrum indeed correspond to transitions from the lowest ($^3H_6$, t_{2g}; 3/2) state to a variety of higher energy $4f^{12}5d^1$ states.

To further analyze the features in the ESE spectra, Figure 3 shows high-resolution ESE spectra. Figure 3a shows onsets of a group of lines at 7100 cm^{-1}, followed by a gap and another group of lines starting at 9000 cm^{-1} (dashed lines). The positions of the onsets are very similar for Tm^{2+} in $CsCaBr_3$ and $CsCaCl_3$. Transitions that involve a different 5d state will strongly depend on the crystal field splitting and vary in energy between a chloride and a bromide. However, transitions involving a rearrangement in the $4f^{12}$ core are expected to be largely independent of the host lattice and this warrants an assignment of the peaks in Figure 3 to transitions within the $4f^{12}$ configuration of the $4f^{12}5d(t_{2g})^1$ state. For a more quantitative comparison, we performed ab initio wave-function-based embedded-cluster calculations for Tm^{2+} in $CsCaBr_3$ and $CsCaCl_3$. A full discussion of the results will be published in a separate paper, but we present the resulting CCDs of the fd states in Figure 4a,b. The details of the calculation methods can be found in the Supporting Information. On the basis of the calculated CCDs, all the sharp peaks in the ESE spectra, starting from 7100 cm^{-1}, are assigned to transitions from the ($^3H_6$, t_{2g}; 3/2) state to mixed ($^3F_4/^1G_4$, t_{2g}) states.

The energy of the $^3H_6 \rightarrow {}^3F_4$ transitions for Tm^{3+} in chlorides is ~5500−6000 cm^{-1}. Clearly, the onset at 7100 cm^{-1} in the experiment and at 7500 cm^{-1} in the calculations is higher in energy than expected based on the $^3H_6$−$^3F_4$ splitting. This observation demonstrates that the energy level structure in the $4f^{12}5d^1$ excited state is not a simple addition of $4f^{12}$ and $5d^1$ splitting. This is in line with earlier experimental observations for $4f^n \rightarrow 4f^{n-1}5d^1$ transitions for trivalent lanthanides in the vacuum UV spectral region. The much richer than expected energy level structure for the simple sum of a $4f^n$ and $5d^1$ splitting is observed and explained by Coulomb and spin−spin interactions between the $4f^{12}$ core and 5d electrons.[19]

A remarkable difference between the one-photon excitation spectra and the excited state absorption spectra is the spectral width of the features observed. The $4f^n \rightarrow 4f^{12}5d^1$ bands in OPE have around 1000 cm^{-1} full width at half-maximum (fwhm), which is typical for f−d transitions. However, in the detailed ESE spectra shown in Figure 3 many sharp lines are observed with spectral widths between 5 and 50 cm^{-1}. The irregular pattern of the positions of the lines in Figure 3c excludes the possibility that the narrow lines are part of a vibronic progression. The lines thus correspond to ZPLs of

DOI: 10.1021/acs.jpclett.6b00924
J. Phys. Chem. Lett. 2016, 7, 2730−2734

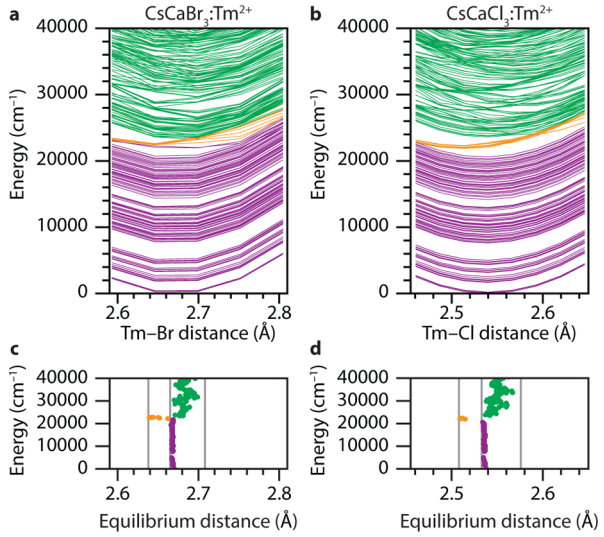

Figure 4. (a,b) Calculated CCDs of the $4f^{12}5d^1$ states in $CsCaBr_3:Tm^{2+}$ and $CsCaCl_3:Tm^{2+}$, corresponding to the gray part of the CCD in Figure 1. The $4f^{12}5d^1(t_{2g})$ parallel PESs at low energy (purple) explain the sharp lines in the ESE, whereas the shifted PESs of mixed $4f^{12}5d^1(t_{2g}/e_g)$ states at higher energy (green) are responsible for broad bands. Also, the impurity trapped excitons (ITE) states (orange) are plotted. (c,d) Equilibrium distances of PESs in (a) and (b). The gray lines show from left to right the equilibrium distances for pure $4f^{12}(ITE)^1$, $4f^{12}5d(t_{2g})^1$, and $4f^{12}5d(e_g)^1$ excited states.

transitions in which there is no change in PES equilibrium position. This is confirmed by the calculated PES equilibrium distances in Figure 4c,d, in which the lowest $4f^{12}5d^1$ states (plotted in purple) have the same equilibrium geometry.

The line widths observed are narrow but still larger than the typical ~1 cm^{-1} inhomogeneous line width observed for $4f^n \leftrightarrow 4f^n$ transitions in crystals. As the quality of the crystals used is high, inhomogeneous broadening for f−f transitions is expected to be less than 1 cm^{-1} and cannot explain the 5−50 cm^{-1} line widths observed. Indeed, narrow (<5 cm^{-1}) emission lines are observed for the $^2F_{5/2}-^2F_{7/2}$ f−f emission of Tm^{2+} in these crystals.[20] We therefore ascribe the large 5−50 cm^{-1} line widths observed here to homogeneous (Heisenberg uncertainty) broadening related to fast relaxation processes to lower energy $4f^{12}5d^1$ states. The density of $4f^{12}5d^1$ states is very high and a fast vibrational relaxation on a picosecond time scale can be expected. Based on the observed spectral widths, the relaxation rates can be estimated to be between 1 ps (5 cm^{-1} fwhm) and 0.1 ps (50 cm^{-1} fwhm). The homogeneous line widths are similar to values reported by Downer for $4f^7 \leftrightarrow 4f^7$ transitions on Eu^{2+} in fluorides.[21] Spectral widths varying from 2 cm^{-1} (for ^6P lines) to 50 cm^{-1} (for ^6D lines) were reported and explained by fast relaxation to a continuum of near resonant, overlapping $4f^65d^1$ states.

Figure 3b shows the part of the spectra where the sharpest lines appear. There is a larger number of peaks in $CsCaBr_3:Tm^{2+}$ than in $CsCaCl_3:Tm^{2+}$, which we ascribe to the lower site symmetry for Tm^{2+} in the bromide (C_i) than in the chloride (C_{4h}), leading to more crystal field components in the bromide.[20,22,23]

At energies above 10 000 cm^{-1} in the ESE spectra, broad bands with a fwhm of hundreds to 1000 cm^{-1} are observed. The broad and structureless nature of these bands indicates that they cannot be assigned by transitions within the $4f^{12}$ configuration of the $4f^{12}5d^1$ excited state but rather to excited states with a PES offset different from the ($^3H_6$, t_{2g}; 3/2) state. However, in the calculated CCD of Figure 4, no such states are found up to 20 000 cm^{-1}, where weakly absorbing impurity trapped excitons (ITE, orange) and mixed $4f^{12}5d(t_{2g}/e_g)^1$ states (green) are found. For the lowest $4f^{12}5d^1$ state, there is a unique situation, with possible absorption by two types of intraconfigurational transitions: f−f transitions within the $4f^{12}$ core and d−d transitions of the electron in the d-orbitals are both possible. Both transitions are parity-forbidden in one-photon absorption but allowed in two-photon absorption (TPA). TPA d−d transitions have a cross section two orders of magnitude larger than TPA f−f transitions.[24,25] The most plausible interpretation of the broad bands in the spectrum is therefore that TPA takes place from the ($^3H_6$, t_{2g}; 3/2) state, resulting in broad bands in the ESE spectra at half the energy of the $4f^{12}5d(t_{2g}/e_g)^1$ states (green lines in Figure 4). There is a good agreement between experiment and calculations on the observed energies. If our hypothesis is correct, this is the first observation of TPA in ESE spectra. Because the strength of TPA scales quadratically with the excitation density,[26] power dependent measurements can be used to verify the assignment.

In summary, we have reported excited state excitation spectra for f−d transitions of Tm^{2+} in $CsCaBr_3$ and $CsCaCl_3$. ESE is a challenging technique that is rarely used, but which provides unique information on excited states that cannot be accessed by one-photon spectroscopy. The rare observation of emission from high energy fd states for Tm^{2+} in $CsCaBr_3$ and $CsCaCl_3$ makes ESE spectroscopy possible for f−d transitions in these systems. The ESE spectra for transitions between different excited $4f^{12}5d^1$ states in Tm^{2+} reveal sharp lines (fwhm ≈ 5−50 cm^{-1}) at low energies and indicate small differences between the Tm^{2+}−ligand equilibrium distance in the potential energy surface for these low-lying fd states. At much higher energies broader ESE bands are observed, reflecting a larger distance offset between the lowest energy $4f^{12}5d(t_{2g})^1$ state and higher energy states. We ascribe the broad bands to TPA by d−d transitions from the lowest $4f^{12}5d(t_{2g})^1$ excited state to mixed $4f^{12}5d(t_{2g}/e_g)^1$ states.

■ ASSOCIATED CONTENT

Supporting Information

The Supporting Information is available free of charge on the ACS Publications website at DOI: 10.1021/acs.jpclett.6b00924.

Additional experimental details and control experiments confirming the starting state of the excited state excitation. (PDF)

■ AUTHOR INFORMATION

Corresponding Author

*E-mail: a.meijerink@uu.nl.

Notes

The authors declare no competing financial interest.

■ ACKNOWLEDGMENTS

We are grateful to Judith Grimm, who synthesized the $CsCaBr_3:Tm^{2+}$ and $CsCaCl_3:Tm^{2+}$ crystals used for the ESE spectra. We acknowledge the helpful suggestions for the figures by Freddy T. Rabouw. The work in this Letter was supported by the EU Marie Curie Initial Training Network LUMINET (316906).

DOI: 10.1021/acs.jpclett.6b00924
J. Phys. Chem. Lett. 2016, 7, 2730−2734

REFERENCES

(1) Blasse, G.; Grabmaier, B. C. *Luminescent Materials*; Springer-Verlag: Berlin, 1994.

(2) Faulkner, S.; Pope, S. J. A.; Burton-Pye, B. P. Lanthanide Complexes for Luminescence Imaging Applications. *Appl. Spectrosc. Rev.* **2005**, *40*, 1−31.

(3) Hong, L.; Mei, Q.; Yang, L.; Zhang, C.; Liu, R.; Han, M.; Zhang, R.; Zhang, Z. Inkjet Printing Lanthanide Doped Nanorods Test Paper for Visual Assays of Nitroaromatic Explosives. *Anal. Chim. Acta* **2013**, *802*, 89−94.

(4) Selvin, P. R. Principles and Biophysical Applications of Lanthanide-Based Probes. *Annu. Rev. Biophys. Biomol. Struct.* **2002**, *31*, 275−302.

(5) Matsuzawa, T.; Aoki, Y.; Takeuchi, N.; Murayama, Y. A New Long Phosphorescent Phosphor with High Brightness, $SrAl_2O_4$:Eu^{2+},Dy^{3+}. *J. Electrochem. Soc.* **1996**, *143*, 2670−2673.

(6) Webb, C. E.; Jones, J. D. C. *Handbook of Laser Technology and Applications − Vol III: Laser Design and Laser Systems*; Institute of Physics Publishing: Bristol, 2004.

(7) Mott, N. F. On the Absorption of Light by Crystals. *Proc. R. Soc. London, Ser. A* **1938**, *167*, 384−391.

(8) Struck, C. W.; Fonger, W. H. Unified Model of the Temperature Quenching of Narrow-Line and Broad-Band Emissions. *J. Lumin.* **1975**, *10*, 1−30.

(9) Barandiarán, Z.; Seijo, L. Quantum Chemical Analysis of the Bond Lengths in f^n and $f^{n-1}d^1$ States of Ce^{3+}, Pr^{3+}, Pa^{4+}, and U^{4+} Defects in Chloride Hosts. *J. Chem. Phys.* **2003**, *119*, 3785−3790.

(10) de Jong, M.; Seijo, L.; Meijerink, A.; Rabouw, F. T. Resolving the Ambiguity in the Relation Between Stokes Shift and Huang-Rhys Parameter. *Phys. Chem. Chem. Phys.* **2015**, *17*, 16959−16969.

(11) Oetliker, U.; Riley, M. J.; May, P. S.; Güdel, H. U. Excitation Avalanche in Ni^{2+}-Doped $CsCdCl_3$. *J. Lumin.* **1992**, *53*, 553−556.

(12) Oetliker, U.; Riley, M. J.; Güdel, H. U. Excited State Spectroscopy of Ni^{2+} Doped Chloride and Fluoride Lattices. *J. Lumin.* **1995**, *63*, 63−73.

(13) Krämer, K. W.; Güdel, H. U.; Schwartz, R. N. NIR to VIS Upconversion in $LaCl_3$: 1% Er^{3+} One- and Two-Color Excitations around 1000 and 800 nm. *J. Alloys Compd.* **1998**, *275*−*277*, 191−195.

(14) Laroche, M.; Girard, S.; Margerie, J.; Moncorgé, R.; Bettinelli, M.; Cavalli, E. Experimental and Theoretical Investigation of the $4f^n \leftrightarrow 4f^{n-1}5d$ Transitions in YPO_4:Pr^{3+} and YPO_4:Pr^{3+},Ce^{3+}. *J. Phys.: Condens. Matter* **2001**, *13*, 765−779.

(15) Peijzel, P. S.; Vermeulen, P.; Schrama, W. J. M.; Meijerink, A.; Reid, M. F.; Burdick, G. W. High-resolution Measurements of the Vacuum Ultraviolet Energy Levels of Trivalent Gadolinium by Excited State Excitation. *Phys. Rev. B: Condens. Matter Mater. Phys.* **2005**, *71*, 125126.

(16) Piramidowicz, R.; Mahiou, R.; Boutinaud, P.; Malinowski, M. Upconversion Excitations in Pr^{3+}-Doped BaY_2F_8 Crystal. *Appl. Phys. B: Lasers Opt.* **2011**, *104*, 873−881.

(17) Reid, M. F.; Senanayake, P. S.; Wells, J. R.; Berden, G.; Meijerink, A.; Salkeld, A. J.; Duan, C.; Reeves, R. J. Transient Photoluminescence Enhancement as a Probe of the Structure of Impurity-Trapped Excitons in CaF_2:Yb^{2+}. *Phys. Rev. B: Condens. Matter Mater. Phys.* **2011**, 113110.

(18) Grimm, J.; Güdel, H. U. Five Different Types of Spontaneous Emission Simultaneously Observed in Tm^{2+} Doped $CsCaBr_3$. *Chem. Phys. Lett.* **2005**, *404*, 40−43.

(19) van Pieterson, L.; Reid, M. F.; Wegh, R. T.; Soverna, S.; Meijerink, A. $4f^n \rightarrow 4f^{n-1}5d$ Transitions of the Light Lanthanides: Experiment and Theory. *Phys. Rev. B: Condens. Matter Mater. Phys.* **2002**, *65*, 045113.

(20) Grimm, J.; Suyver, J. F.; Beurer, E.; Carver, G.; Güdel, H. U. Light-Emission and Excited-State Dynamics in Tm^{2+} Doped $CsCaCl_3$, $CsCaBr_3$, and $CsCaI_3$. *J. Phys. Chem. B* **2006**, *110*, 2093−2101.

(21) Downer, M. C.; Cordero-Montalvo, C. D.; Crosswhite, H. Study of New $4f^7$ Levels of Eu^{2+} in CaF_2 and SrF_2 Using Two-Photon Absorption Spectroscopy. *Phys. Rev. B: Condens. Matter Mater. Phys.* **1983**, *28*, 4931−4943.

(22) Vaills, Y.; Buzaré, J. Y.; Gibaud, A.; Launay, C. X-Ray Investigations of the Cubic to Tetragonal Phase Transition in $CsCaCl_3$ at T_c = 95 K. *Solid State Commun.* **1986**, *60*, 139−141.

(23) Seifert, H. J.; Haberhauer, D. Über die Systeme Alkalimetall-bromid/Calciumbromid. *Z. Anorg. Allg. Chem.* **1982**, *491*, 301−307.

(24) Dalzell, C. J.; Han, T. P. J.; Ruddock, I. S. The Two-Photon Absorption Spectrum of Ruby and its Role in Distributed Optical Fibre Sensing. *Appl. Phys. B: Lasers Opt.* **2011**, *103*, 113−116.

(25) Downer, M. C.; Bivas, A. Third- and Fourth-Order Analysis of the Intensities and Polarization Dependence of Two-Photon Absorption Lines of Gd^{3+} in LaF_3 and Aqueous Solution. *Phys. Rev. B: Condens. Matter Mater. Phys.* **1983**, *28*, 3677−3696.

(26) Göppert-Mayer, M. Über Elementarakte mit zwei Quantensprüngen. *Ann. Phys. (Berlin, Ger.)* **1931**, *401*, 273−294.

DOI: 10.1021/acs.jpclett.6b00924
J. Phys. Chem. Lett. 2016, 7, 2730−2734